

Structural chemistry involved in information detection and transmission by gas sensor heme proteins: Resonance Raman investigation*

Samir F. El-Mashtoly¹ and Teizo Kitagawa^{2,‡}

¹Department of Chemistry, Faculty of Science, King Khalid University, Abha 9004, Saudi Arabia; ²Toyota Physical and Chemical Research Institute, Nagakute, Aichi 480-1192, Japan

Abstract: A variety of heme-containing gas sensor proteins have been discovered by gene analysis from bacteria to mammals. In general, these proteins are composed of an N-terminal heme-containing sensor domain and a C-terminal catalytic domain. Binding of O₂, CO, or NO to the heme causes a change in the structure of heme, which alters the protein conformation in the vicinity of the heme, and the conformational change is propagated to the catalytic domain, leading to regulation of the protein activity. This mini-review summarizes the recent resonance Raman studies obtained with both visible and UV excitation sources for two O₂ sensor proteins, *EcDOS* and *HemAT-Bs*. These investigations have shown the role of heme propionate hydrogen-bonding interactions in communicating the heme structural changes, which occur upon ligand binding, from heme to the protein moiety. Furthermore, it is deduced that the contact interactions between the heme 2-vinyl group and the surrounding residues are also important for signal transmission from heme to protein in *EcDOS*.

Keywords: gas sensor proteins; resonance Raman; *EcDOS*; *HemAT-Bs*; heme propionate.

INTRODUCTION

Sensory proteins have physiological functions that enable cells to respond to external stimuli such as light, voltage, and chemicals. Some of these proteins use cofactors to help in the detection of their input signal. For instance, heme-based gas sensor proteins use heme cofactors in the detection of O₂, CO, or NO [1–6]. In general, these proteins are composed of an N-terminal heme-containing sensor domain and a C-terminal functional domain. The binding of O₂, CO, or NO to the heme changes the structure of heme, which alters the protein conformation in the heme vicinity, and the conformational change is propagated to the functional domain, leading to regulation of the protein activity. Representative proteins in this category discovered so far are listed in Table 1. A heme-bound PAS is included in several sensor proteins such as FixL from *Rhizobium*, phosphodiesterase A1 from *Acetobacter xylinum*

*Paper based on a presentation at the International Symposium on Metallomics 2007 (ISM 2007), 28 November–1 December 2007, Nagoya, Japan. Other presentations are published in this issue, pp. 2565–2750.

‡Corresponding author: Tel.: +81-80-1620-8159; Fax: +81-561-63-6302; E-mail: Riken-kitagawa@mosk.tytlabs.co.jp

(AxPDEA1)*, direct oxygen sensor from *Escherichia coli* (EcDOS), and neural PAS domain protein 2 (NPAS2).

Table 1 Representative heme-based gas sensor proteins.

Target	Protein	Function	Source
CO	CooA	Transcriptional factor	<i>Rhodospirillum rubrum</i>
CO	NPAS2	Transcriptional factor	Mammalian brain
NO	sGC	Conversion of GTP to c-GMP	Mammalian brain, lung, etc.
O ₂	FixL	Kinase	<i>Rhizobium meliloti</i>
O ₂	DOS	Phosphodiesterase	<i>Escherichia coli</i>
O ₂	PDEA1	Phosphodiesterase	<i>Acetobacter xylinum</i>
O ₂	HemAT	Signal transducer for aerotaxis	<i>Bacillus subtilis</i>
O ₂	DosS	Kinase	<i>Mycobacterium tuberculosis</i>
O ₂	DosT	Kinase	<i>Mycobacterium tuberculosis</i>

CooA and NPAS2 are CO-sensing proteins. CooA is a transcriptional factor from *Rhodospirillum rubrum* that contains a CO-bound heme sensor domain and regulates the expression of the *coo* genes associated with CO-dependent production of proteins [7–9]. NPAS2 is also a transcriptional factor, but unlike CooA, it contains two heme-bound PAS domains in its N-terminus, and it binds to DNA along with BMAL1 and regulates the circadian rhythm [10]. Soluble guanylate cyclase (sGC), which is a NO sensor protein, catalyzes the conversion of guanosine triphosphate (GTP) to cyclic guanosine monophosphate (c-GMP), an intracellular second messenger [11–13].

The O₂-sensing proteins identified so far include FixL, AxPDEA1, EcDOS, MtDos, and HemAT. FixL is an O₂ sensor protein that contains a heme-bound PAS domain as a sensor. The catalytic domain of FixL serves as a protein kinase that phosphorylates the FixJ protein, which regulates the expression of nitrogen fixation gene [14–16]. FixL is inactivated when O₂ binds to the heme of FixL, and this is a mechanism that protects the nitrogen fixation proteins from oxidative damage. AxPDEA1 has also a heme-bound PAS domain as a sensor, and it catalyzes the hydrolysis of 3',5'-cyclic diguanylic acid (c-di-GMP), which is required for the activation of cellulose synthase in cellulose-producing bacteria [17]. The MtDos is an O₂ sensing system recently obtained from *Mycobacterium tuberculosis* and consists of a cognate response regulator, DosR and two-component O₂-dependent histidine kinase, DosS and DosT [18–21]. DosR induces a regulon consisting of around 50 proteins such as α -crystallin, which is the major cell-wall protein in stationary-phase bacteria, and is associated with dormancy [22,23]. This system (Dos S/T/R) is hypothesized to mediate the entry of this pathogen into dormancy and to adjust the system along the environmental stimuli such as hypoxia and NO.

HemAT is a heme-based signal transducer protein responsible for bacterial aerotaxis [24–28]. The HemAT monomer consists of two domains, a sensor domain and a signaling domain. The sensor domain has globin folds containing a heme that acts as the O₂ binding site. The signaling domain of HemAT interacts with a histidine kinase protein CheA, a component of the CheA/CheY two component signal transduction system that regulates a rotation direction of the flagellar motor [29–31].

*The abbreviations used are: AxPDEA1, phosphodiesterase A1 protein from *Acetobacter xylinum*; EcDOS, direct oxygen sensor from *Escherichia coli*; EcDOSH, isolated heme domain of EcDOS; PDE, phosphodiesterase; c-di-GMP, 3',5'-cyclic diguanylic acid; HemAT-Bs, HemAT from *Bacillus subtilis*; UVR, ultraviolet resonance Raman; WT, wild-type; PAS, an acronym formed from the names of proteins in which imperfect repeat sequences were initially recognized: PER, the *Drosophila* period clock protein; ARNT, vertebrate aryl hydrocarbon receptor nuclear translocator; SIM, *Drosophila* single-minded protein; TR³, time-resolved resonance Raman; Mb, myoglobin.

EcDOS is composed of a heme-bound PAS domain as a sensor, and a PDE catalytic domain. As *EcDOS* shows high sequence similarity to the heme domain of FixL, it was proposed to be a direct oxygen-sensing protein as well [32]. However, Sasakura and coworkers found that *EcDOS* exhibits PDE activity toward c-AMP, in a redox-dependent manner, and that the enzyme is active when the heme is in the reduced form but inactive when the heme is oxidized [33]. Recently, however, its role as a general gas sensor has also been put forward on the basis of moderate up-regulation of activity by CO, NO, and O₂ toward c-di-GMP [34,35].

Resonance Raman (RR) spectroscopy is a powerful technique for studying heme proteins [36]. In the visible excited RR spectra, several marker bands that are sensitive to the oxidation, coordination, and spin states of heme are known [36–38]. Furthermore, assignments of the vibrational modes of heme-peripheral side chains as well as iron-ligand and ligand internal stretching modes have been established for exogenous ligands [39,40]. These bands are useful for the structural characterization of the heme and its environment in proteins. When the excitation wavelength is within the UV region between 220–250 nm, the vibrational spectra of the aromatic side chains such as Tyr and Trp residues are selectively obtained [41–43]. This would provide structural information about their conformations, local environments, and hydrogen-bonding interactions. Such kinds of specific information have been proved to be essential to understand the structural mechanisms of a variety of heme proteins and other chromoproteins [44–47].

Elucidation of the communication pathway between heme and protein moiety is important to understand the chemistry of heme-sensor proteins. Recently, we have investigated this pathway with myoglobin (Mb) as a model for gas sensory heme proteins by using UVRR spectroscopy. Figure 1 displays the hydrogen-bonding networks in the vicinity of heme in Mb as revealed by Bartunik's group with X-ray crystallography [48]. The proximal His (His-93) forms hydrogen bonds with Ser92 and Leu89. The heme 7-propionate forms hydrogen bonds with His97 and Ser92, whereas the heme 6-propionate participates in a hydrogen-bonding network with Arg45, H₂O, and His-64. We have found that the mutations of the nearby residues or chemical modification of the propionate side chain of heme significantly changes the conformation of Trp residues in the A helix of the globin, which are far from the heme in Mb. It is deduced from this study that heme structural changes upon ligand binding in Mb are communicated to the globin through heme propionates in addition to the Fe–His bond [45]. Accordingly, in this mini-review, we discuss specificity in gas-sensing and how the heme structural changes occurring upon ligand binding/dissociation are transmitted from heme to the protein moiety in the heme sensor domain and afterwards to the catalytic/signaling domain in both *EcDOS* and HemAT-*Bs* proteins.

STRUCTURAL CHARACTERIZATION OF THE HEME ACTIVE SITE OF GAS SENSOR *EcDOS* PROTEIN

The N-terminal of *EcDOS* consists of a heme-containing domain (residues 21–133, *EcDOS*H) and a heme-free domain (residues 141–256). The RR spectra for heme of the *EcDOS*H domain indicated that heme in both oxidized and reduced forms adopts six-coordinate low-spin states (6c-1s) [49–51]. Figure 2 depicts the visible excited RR spectra of the oxidized (a) and reduced (b) forms of the full-length *EcDOS*. They reflect the vibrations of the heme in *EcDOS*. The Raman bands of the oxidized form at 1371, 1506, 1578, and 1641 cm⁻¹ (a) are assigned to ν_4 , ν_3 , ν_2 , and ν_{10} , respectively, and their frequencies indicate that the heme adopts a 6c-1s state. The ν_4 , ν_3 , and ν_2 , and ν_{10} bands of the reduced form (b) are observed at 1362, 1494, and 1581 cm⁻¹, respectively, suggesting a 6c-1s type of heme. These spectra are similar to those of *EcDOS*H domain [49–51], implying that the PDE domain hardly affect the heme environment. In addition, by using RR spectroscopy in combination with site-directed mutagenesis, it is proposed that His77 and Met95 residues are the heme axial ligands in the reduced form of *EcDOS*H [33,50,52] and Met95 is displaced upon binding of an external ligand (O₂, CO, or NO) to the heme.

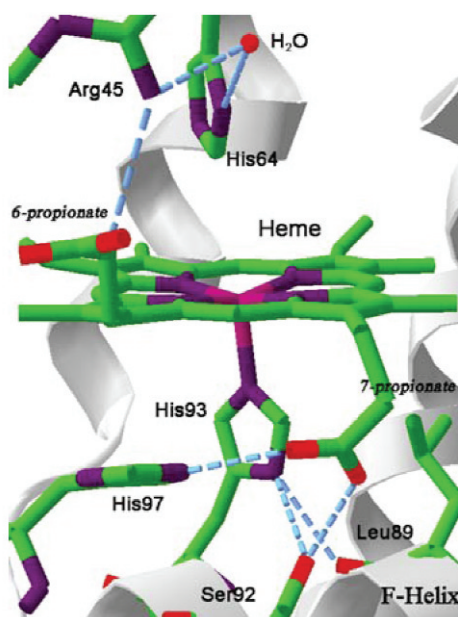


Fig. 1 Hydrogen-bonding network in the vicinity of heme of Mb [48]. Reprinted from ref. [45]. Copyright © 2006 American Society for Biochemistry and Molecular Biology.

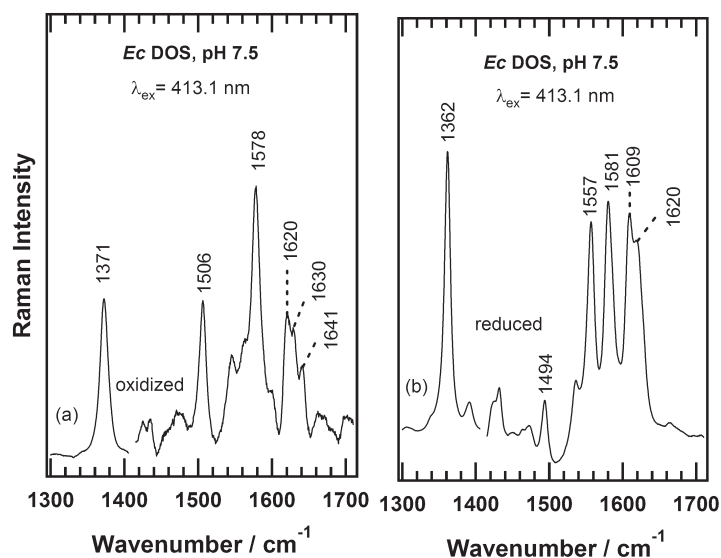


Fig. 2 RR spectra of the full-length WT *Ec*DOS of the oxidized (a) and reduced (b) forms excited at 413.1 nm. The sample concentration was 100 μ M in 50 mM Tris-HCl buffer, pH 7.5.

The $\nu_{\text{Fe-O}_2}$ band in the RR spectrum of O_2 -bound form is observed at 561 cm^{-1} . This frequency is lower than that of Mb and suggesting that heme-bound O_2 forms a strong hydrogen bond with nearby residue [50]. On the other hand, for the CO- and NO-bound forms, both the hydrogen- and non-hydrogen-bonded conformations were coexisting and in the former Arg97 forms a hydrogen bond with the heme-bound external ligand [53].

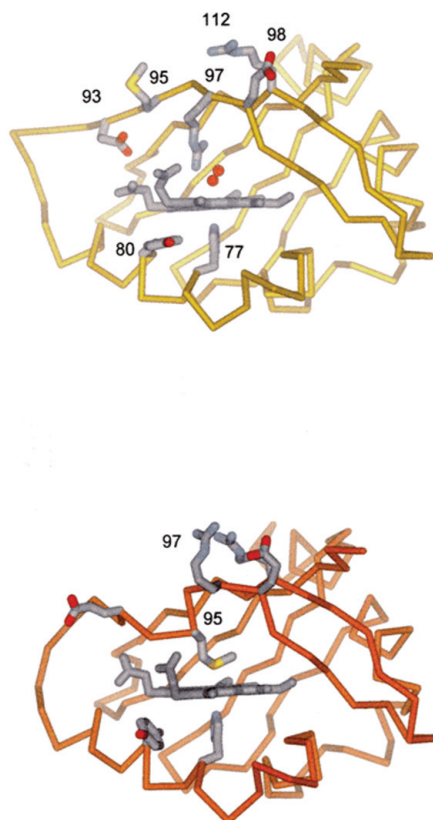


Fig. 3 X-ray structure of the *EcDOSH* (PDB ID: 1S66; ref. [55]). The heme environment is shown for both O₂-bound (upper) and reduced (lower) forms. Copyright © 2004 American Chemical Society.

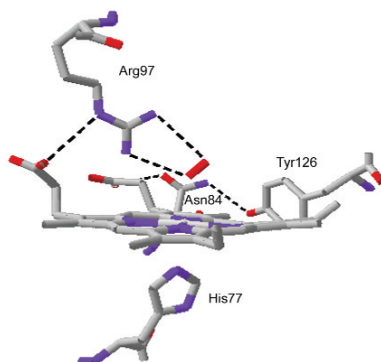


Fig. 4 X-ray structure of the O₂-bound *EcDOSH* protein (PDB ID: 1S66; ref. [55]). Hydrogen bond networks around iron-bound O₂ and heme propionates of *EcDOSH* are displayed with broken lines. Copyright © 2007 American Chemical Society.

The O₂-bound form was changed to the oxidized form due to autoxidation. The RR spectrum of oxidized form was also of 6c-1s type and remained unchanged between pH 4.4 and 10.0 [50]. Thus, the sixth ligand in the oxidized form would be strongly hydrogen-bonded water. Strongly hydrogen-bonded water would be close to OH⁻ and therefore, may yield 6c-1s state in heme.

Recently, the X-ray crystallographic structures of the reduced, oxidized, and O₂-bound forms of the *Ec*DOSH were determined and confirmed the structures deduced from RR spectra mentioned above [54,55]; Met95 is an endogenous axial ligand of the reduced heme which is replaced by O₂ in the O₂-bound form, but is replaced by H₂O (or OH⁻) in the oxidized form (Fig. 3). Furthermore, Arg97 forms strong hydrogen bonds with heme-coordinated O₂. Similar switching of the heme axial ligand accompanied by a redox change or binding of an external ligand has been reported for other heme sensor proteins such as CooA, a CO sensor protein, in which the heme axial ligands in the reduced form are His77 and Pro2 and those in the oxidized form are Cys75 and Pro2. In this case, Pro2 is replaced by an exogenous CO molecule to allow binding to DNA [56].

As Arg97 in the heme distal side of *Ec*DOS interacts with heme-bound O₂ after Met95 is replaced by O₂, the effect of mutating these residues on the PDE activity and the target specificity of *Ec*DOS has been explored [35]. Tanaka et al. found that R97A, R97I, and R97E mutations do not significantly affect the regulation of the PDE activities by CO- and NO-binding. The PDE activities of the O₂ bound form of the mutants could not be determined due to rapid autoxidation and/or low affinity for O₂ [35]. In contrast, the activities of the gas-free M95A and M95L mutants were similar to that of the gas-activated WT protein. Interestingly, the activity of the M95H mutant was partially enhanced by O₂, CO, and NO [35]. Spectroscopic analysis indicated that the reduced heme in the M95A and M95L mutants is in the 5-coordinated high-spin state (5c-hs) but that in the M95H mutant is in the 6c-1s state like that in WT *Ec*DOS [50,52,57]. These results suggest that Met95 coordination to the reduced heme is critical for locking the system and that global structural change around Met95 caused by the binding of the external ligands or mutations at Met95 releases the catalytic lock and activates catalysis [35].

Liebl and coworkers [58] reported the CO-rebinding kinetics upon its photodissociation for WT *Ec*DOSH. They showed that Met95 binding to the heme occurs in 100 μs in competition with bimolecular CO recombination and is followed by subsequent replacement of Met95 by CO around 8 ms [58]. The mutation of Met95 and Arg97 significantly perturbs the dynamics of *Ec*DOSH as indicated by the time-resolved RR (TR³) results [53]. Specifically, in the absence of Met95, CO begins to rebind to the heme near 100 μs. In R97I mutant, however, Met95 does not bind to the heme but CO rebinds. In R97E mutant on the other hand, Met95 binding is much slower compared with that observed for WT, implying that the negative charge in side chains of Glu97 in R97E probably raises the potential barrier for re-binding of CO. It is deduced from these results that the electrostatic interactions of Arg97 with the heme-bound ligand in *Ec*DOSH would be crucial for regulating the binding of sixth ligand of heme. In addition, the TR³ results for Phe113 mutants also suggested that the steric but not polar interactions of Phe113 in the heme distal site are critical for the Met95 binding to the heme prior CO recombination [53].

COMMUNICATION PATHWAY BETWEEN HEME AND PROTEIN IN *Ec*DOS

The crystal structure of the O₂-bound form shows that Trp53 and Tyr126 are located near the 2-vinyl and 4-vinyl side chains, respectively. In addition, heme 6-propionate constitutes a hydrogen bond network with Asn84 and Tyr126 (Fig. 4). In fact, we have recently demonstrated that UVRR spectroscopy is an ideal technique for monitoring conformational changes occurring upon ligand binding or redox change through vibrational spectra of these aromatic residues in the heme surroundings [59,60]. For instance, the UVRR results indicate that most of Trp and Tyr residues experience spectral changes upon ligand binding or redox change. Specifically, Trp53 and Tyr55, which are present near the 2-vinyl side chain, experiences environmental changes upon ligand binding or redox change [59,60]. The visible-excited RR spectra also indicate that heme 2-vinyl group in *Ec*DOSH undergo significant spectral changes upon ligand binding or redox change. This implies that the interactions of heme 2-vinyl group with the surroundings in *Ec*DOSH protein are altered by the ligand binding or redox change [60]. Consequently, it is reasonable to suggest that the heme structural changes are communicated through

the 2-vinyl group to Trp53 and Tyr55 in the heme proximal side upon ligand binding or heme reduction.

Consistent with these results, the mutation of Trp53 and Tyr55 significantly perturbed the PDE activities of the full-length *EcDOS*. Specifically, the activity of W53F is decreased by ~65 and 24 % in the ligand bound and oxidized forms, respectively, compared with those of WT [59]. In addition, the activity of Y55F is reduced by ~45 and 12 % in the oxidized and reduced forms, respectively, compared with those of WT, while the activity is enhanced by ~37 and 10 % upon the binding of CO and O₂, respectively, compared with those of WT [60]. These results are important and may be related to signal transduction mechanism of *EcDOS*, where Trp53 and Tyr55 are located near the Glu59-Lys104 salt bridge at the surface of the sensor domain. This salt bridge is well conserved on the surface of general PAS proteins, and it was proposed that the salt bridge plays an important role in the signal transduction [61].

The UVRR results indicated that Tyr residues suffer large spectral changes upon ligand binding. Most of these changes were assigned to Tyr126, which forms a hydrogen bond with Asn84 and heme 6-propionate in O₂-bound form. Thus, large changes in heme 6-propionate hydrogen-bonding network occur upon ligand binding. The mutation of Asn84 abolishes the UVRR spectral changes observed for WT upon O₂-binding [59]. Thus, Asn84 forms a hydrogen bond with Tyr126 in O₂-bound form but not in the reduced form. In fact, the visible-excited RR spectra of WT showed that the deformation vibration of heme propionate changes from 376 cm⁻¹ in the ligand-free form to 383 cm⁻¹ in the O₂-bound form, indicating that the propionate side chains are significantly influenced upon O₂ binding [50,60]. Indeed, the crystal structures of the reduced and O₂ forms of WT show that both of two propionates side chains of heme rotate upon ligand switch from Met95 to O₂ [55]. The rotation of the 7-propionate side chain is accompanied by rearrangement of the hydrogen-bonding network including Arg97 and heme-bound O₂. The rotation of the 6-propionate side chain may trigger the formation of the hydrogen bond network between Asn84 and Tyr126 through the heme 6-propionate in the O₂-bound form (Fig. 4).

Furthermore, it was shown that the cleavage of the Asp40-Arg85 salt bridge of *EcDOS* by mutation of Asp40 abolished the PDE activity toward c-AMP [62]. Arg85 is an immediate neighborhood of Asn84 (F-helix) and also contacts Tyr126 (I_β). Thus, the alteration in the heme 6-propionate hydrogen-bonding network is expected to communicate the conformational changes from F-helix to I_β strand on the surface of the sensor domain. Consistent with this idea, the PDE activities for the ligand-bound forms of N84V and Y126F mutants toward c-di-GMP are decreased by ~46–68 % compared with that of WT [59]. Therefore, a part of the conformational changes that occur to the sensor domain upon ligand binding propagate to the PDE domain through the heme 6-propionate hydrogen-bonding network, leading to the regulation of the enzymatic activity.

STRUCTURAL CHARACTERIZATION OF THE HEME ACTIVE SITE OF O₂ SENSOR HemAT-*Bs* PROTEIN

The X-ray structures of the reduced unligated and oxidized cyanide-bound forms of the truncated sensor domain of HemAT-*Bs* were determined [63]. The sensor domain protein maintains classic globin folds and forms a homodimer. The active site of the sensor domain of the CN-bound form contains a unique distal heme pocket surrounded by Tyr70, Thr95, and a water molecule. Because Tyr70 exhibits distinct conformational changes in one subunit of the dimer when the ligand is removed, the symmetry breaking of HemAT-*Bs* was proposed to play an important role in initiating the chemotaxis signal transduction cascade [63]. The roles of the distal residues in the sensing mechanism of HemAT-*Bs* were further investigated by RR spectroscopy in combination with site-directed mutagenesis [64,65].

We reported for the O₂-bound WT HemAT-*Bs* that there are three O₂-isotope sensitive bands ($\nu_{\text{Fe-O}_2}$) at 554, 566, and 572 cm⁻¹ [64]. The band at 554 cm⁻¹ is deduced to arise from the species with strong hydrogen bonds between the proximal and distal oxygen atoms of heme-bound O₂ and a protein residue. The frequency of 566 cm⁻¹ implies the presence of moderately strong hydrogen bond between

the distal oxygen atom of heme-bound O₂ and a protein residue, and the $\nu_{\text{Fe-O}_2}$ at 572 cm⁻¹ corresponds to open form conformation in which the heme-bound oxygen does not form a hydrogen bond with the surroundings. In addition, the visible-excited RR results demonstrated that T95A mutant has a single conformation of the distal heme pocket, which would correspond to the open form with $\nu_{\text{Fe-O}_2}$ at 572 cm⁻¹ [64]. Thus, Thr95 is essential to maintain the closed form. In contrast, the mutation of Tyr70 causes little effect on $\nu_{\text{Fe-O}_2}$ bands. Therefore, it is proposed that Thr95 forms hydrogen bond with heme-bound O₂ but Tyr70 does not.

The bending mode of the heme propionate, $\delta(\text{C}_\beta\text{C}_\epsilon\text{C}_\delta)$, in the RR spectra of O₂-bound HemAT-*Bs* is observed at 370 and 383 cm⁻¹, suggesting that there are two species with different conformations around the heme propionates or that the two propionates of a single heme have different geometry [65]. The propionate-bending frequencies are correlated with the strength of the hydrogen bond between heme propionate and the surrounding amino acid residues [66–68]. The stronger the hydrogen-bonding interactions, the higher the frequency of the $\delta(\text{C}_\beta\text{C}_\epsilon\text{C}_\delta)$ band. The $\delta(\text{C}_\beta\text{C}_\epsilon\text{C}_\delta)$ band at 370 cm⁻¹ in the O₂-bound HemAT-*Bs* is lower than that of Mb in which moderate strength hydrogen bonds exist on heme 7-propionate [69]. Thus, the conformer displaying this band has no hydrogen bond or a weak hydrogen bond on the heme propionate. On the other hand, the additional $\delta(\text{C}_\beta\text{C}_\epsilon\text{C}_\delta)$ band at 383 cm⁻¹ in O₂-bound HemAT-*Bs* indicates the presence of a stronger hydrogen bond between the heme propionate and the surrounding residue. This conformer was observed only for the O₂-bound but not for CO- and NO-bound forms. The propionate bending mode at 383 cm⁻¹ in the O₂-bound form of HemAT-*Bs* disappeared by mutation of only His86. Therefore, we proposed that His86 forms a hydrogen bond with heme 6-propionate only in the O₂-bound form [65].

Furthermore, the Fe–O₂ stretching frequency of H86A HemAT-*Bs*, for which the band at 566 cm⁻¹ disappeared but the bands at 557 and 572 cm⁻¹ were observed, was also different from that of WT HemAT-*Bs*. These results indicate that the loss of the hydrogen bond between His86 and heme 6-propionate affects the hydrogen-bonding interaction between the heme-bound O₂ and Thr95. Therefore, Yoshimura et al. proposed that His86 forms a hydrogen bond with a heme 6-propionate upon binding of O₂ to the heme [65]. This hydrogen bond formation induces conformational changes of the protein by which Thr95 is moved to a position suitable to form a hydrogen bond with the heme-coordinated O₂, while Tyr70 does not form a hydrogen bond with the heme-bound O₂.

COMMUNICATION PATHWAY BETWEEN HEME AND PROTEIN IN HemAT-*Bs*

Full-length HemAT-*Bs* protein contains a single Trp (Trp132) and six Tyr (Tyr13, Tyr49, Tyr70, Tyr133, Tyr148, and Tyr184) residues. Trp132 and Tyr133 are located in the proximal side of heme, but Tyr70 in the distal side, while Tyr49, Tyr148, and Tyr184 residues are far from the heme (Fig. 5A). Only Tyr184 stays in the linker region between the sensor and the signaling domains. The UVRR results demonstrated that Raman intensities of Trp132 and some Tyr residues change upon binding of different ligands, but no frequency shift is observed for the UVRR bands [70]. These results imply that Trp132 and some Tyr residues undergo appreciable environmental changes in hydrophobicity upon ligand binding. The UVRR results of Tyr mutants suggested that Tyr70 in the heme distal side and Tyr133 in the heme proximal side undergo hydrophobicity change upon ligand binding. Thus, both Trp132 and Tyr133 from G-helix in the heme proximal side suffer environmental changes upon ligand binding. Furthermore, it is suggested from the spectral comparison between the full-length and truncated sensor domain proteins of HemAT-*Bs* that Tyr184 in the linker region exhibits small spectral change upon ligand binding, and the magnitude of its change seems to depend on a ligand species. This implies that conformational change of the sensor domain upon ligand binding is communicated to the signaling domain through the linker region [70].

Yoshimura et al. proposed that a hydrogen bond is formed between His86 and heme 6-propionate only when O₂ is bound to the heme [65]. The formation of this hydrogen bond induces conformational

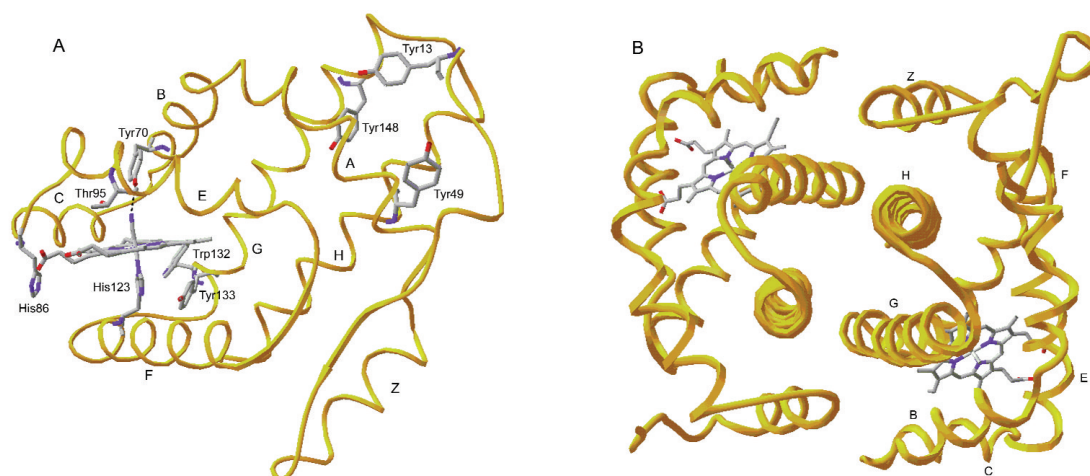


Fig. 5 X-ray structure of the CN-bound form of truncated HemAT-*Bs* protein (PDB ID: 1OR4; ref. [63]). The heme, Trp, Tyr, His86, Thr95, and His123 residues are explicitly represented in Panel A, where a hydrogen bond between Tyr70 and heme bound-CN is depicted by a black broken line. Panel B shows the top view of the same protein, which exhibits the flanking of the core helices, G, and H (four helix bundle). The helices are labeled in accord with the nomenclature of the globin fold. Reprinted from ref. [70]. Copyright © 2008 American Society for Biochemistry and Molecular Biology.

change in the heme distal side, by which Thr95 is displaced to a proper position to form a hydrogen bond with the bound-O₂. We have investigated the role of these hydrogen bonds in communicating the heme structural changes which occur upon ligand binding, to the protein moiety. It is deduced from this study that the removal of these hydrogen bonds in H86A and T95A mutants strongly perturb the conformational changes of Tyr70 (B-helix), Tyr133, and Trp132 (G-helix) in both the distal and proximal sides of heme. Therefore, the UVRR results suggest that hydrogen bonds between Thr95 and heme-bound O₂ and between His86 and heme 6-propionate in HemAT-*Bs* substantially contribute to communicate the structural changes of heme to the protein moiety in both B- and G-helices upon O₂-binding [70].

The conformational changes of G-helix residues are quite important and may be related to the signal transduction mechanism of HemAT-*Bs*. The G and H helices of the two subunits of homo-dimer form an antiparallel four-helical bundle (Fig. 5B) and lie in the C-terminal region (the sensor domain), and the H helices are apparently continuous to the extended helical structure of the signaling domain. The crystal structure showed small displacements of the four-helical bundle upon CN-binding [63]. If similar displacements of the helical bundle occur upon O₂ binding, it would trigger the transduction of the conformational changes from the sensor domain to the signaling domain. Such helical bundle movement mechanism has been proposed for methyl-accepting chemotaxis protein [71,72].

CONCLUDING REMARKS

Heme-based sensors are a class of allosteric proteins which regulate the enzymatic and DNA- and protein-binding activities in response to the presence of diatomic target molecules like CO, NO, or O₂. In this mini-review, we have discussed the RR spectroscopic results of *EcDOS* and HemAT-*Bs* proteins, obtained in both visible and UV excitation sources in order to reveal (1) heme structural change upon ligand binding, (2) conformational changes which occur to the protein moiety, and (3) how signal is transmitted from heme to protein. The visible excited RR spectra have revealed that heme propionates in both *EcDOS* and HemAT-*Bs* experience structural changes upon ligand binding. Specifically, the hy-

drogen-bonding interactions of the heme propionates are altered in the O₂-bound form. Heme 2-vinyl group also suffers large changes upon ligand binding or redox change in EcDOS. Furthermore, the UVRR results have shown that some aromatic residues which are located near to and far from the heme undergo environmental changes upon ligand binding. Finally, the UVRR spectroscopy in combination with site-directed mutagenesis demonstrated how the signal is transmitted from the heme to those aromatic residues upon ligand binding.

ACKNOWLEDGMENTS

We are grateful to our collaborators, Prof. Toru Shimizu, Dr. Hirofumi Kurokawa, Dr. Hiroto Takahashi, and Dr. Atsunari Tanaka for the work on EcDOS and Prof. Shigetoshi Aono, Dr. Hideaki Yoshimura, and Dr. Shiro Yoshioka for the work on HemAT-Bs. This study was supported by a JSPS Fellowship to S.F. E.-M. from the Japan Society for the Promotion of Science and by a Grant-in-Aid for Basic Scientific Research to T.K. (19350089) from the Japan Society for the Promotion of Science.

REFERENCES

1. K. R. Rodgers. *Curr. Opin. Chem. Biol.* **3**, 158 (1999).
2. M. K. Chan. *Curr. Opin. Chem. Biol.* **5**, 216 (2001).
3. S. Aono, H. Nakajima. *Coord. Chem. Rev.* **190–192**, 267 (1999).
4. M.-A. Gilles-Gonzalez, G. Gonzalez. *J. Inorg. Biochem.* **99**, 1 (2005).
5. T. Uchida, T. Kitagawa. *Acc. Chem. Res.* **38**, 662 (2005).
6. Y. Sasakura, T. Yoshimura-Suzuki, H. Kurokawa, T. Shimizu. *Acc. Chem. Res.* **39**, 37 (2006).
7. D. Shelver, R. L. Kerby, Y. He, G. P. Roberts. *J. Bacteriol.* **177**, 2157 (1995).
8. S. Aono, H. Nakajima, K. Saito, M. Okada. *Biochem. Biophys. Res. Commun.* **228**, 752 (1996).
9. S. Aono. *Acc. Chem. Res.* **36**, 825 (2003).
10. E. M. Dioum, J. Rutter, J. R. Tuckerman, G. Gonzalez, M. A. Gilles-Gonzalez, S. L. McKnight. *Science* **298**, 2385 (2002).
11. I. Ruiz-Stewart, S. R. Tiyyagura, J. E. Lin, S. Kazerounian, G. M. Pitari, S. Schulz, E. Martin, F. Murad, S. A. Waldman. *Proc. Natl. Acad. Sci. USA* **101**, 37 (2004).
12. M. Russwurm, D. Koesling. *EMBO J.* **23**, 4443 (2004).
13. E. M. Boon, S. H. Huang, M. A. Marletta. *Nat. Chem. Biol.* **1**, 53 (2005).
14. M. A. Gilles-Gonzalez, G. S. Ditta, D. R. Helinski. *Nature* **350**, 170 (1991).
15. W. Gong, B. Hao, S. S. Mansy, G. Gonzalez, M. A. Gilles-Gonzalez, M. K. Chan. *Proc. Natl. Acad. Sci. USA* **95**, 15177 (1998).
16. H. Nakamura, H. Kumita, K. Imai, T. Iizuka, Y. Shiro. *Proc. Natl. Acad. Sci. USA* **101**, 2742 (2004).
17. A. L. Chang, J. R. Tuckerman, G. Gonzalez, R. Mayer, H. Weinhouse, G. Volman, D. Amikam, M. Benziman, M.-A. Gilles-Gonzalez. *Biochemistry* **40**, 3420 (2001).
18. D. R. Sherman, M. Voskuil, D. Schnappinger, R. Liao, M. I. Harrell, G. K. Schoolnik. *Proc. Natl. Acad. Sci. USA* **98**, 7534 (2001).
19. M. I. Voskuil, D. Schnappinger, K. C. Visconti, M. I. Harrell, G. M. Dolganov, D. R. Sherman, G. K. Schoolnik. *J. Exp. Med.* **198**, 705 (2003).
20. E. Henrique, S. Sousa, J. R. Tuckerman, G. Gonzalez, M.-A. Gilles-Gonzalez. *Protein Sci.* **16**, 1708 (2007).
21. D. K. Saini, V. Malhotra, D. Dey, N. Pant, T. K. Das, J. S. Tyagi. *Microbiology* **150**, 865 (2004).
22. A. F. Cunningham, C. L. Spreadbury. *J. Bacteriol.* **180**, 801 (1998).
23. B. Y. Lee, S. A. Hefta, P. J. Brennan. *Infect. Immun.* **60**, 2066 (1992).
24. S. Hou, R. W. Larsen, D. Boudko, C. W. Riley, E. Karatan, M. Zimmer, G. W. Ordal, M. Alam. *Nature* **403**, 540 (2000).

25. S. Hou, T. Freitas, R. W. Larsen, M. Piatibratov, V. Sivozhelezov, A. Yamamoto, E. A. Meleshkevitch, M. Zimmer, G. W. Ordal, M. Alam. *Proc. Natl. Acad. Sci. USA* **98**, 9353 (2001).
26. S. Aono, T. Kato, M. Matsuki, H. Nakajima, T. Ohta, T. Uchida, T. Kitagawa. *J. Biol. Chem.* **277**, 13528 (2002).
27. W. Zhang, J. S. Olson, G. N. Phillips. *Biophys. J.* **88**, 2801 (2005).
28. T. Ohta, T. Kitagawa. *Inorg. Chem.* **44**, 758 (2005).
29. H. Szurmant, G. W. Ordal. *Microbiol. Mol. Biol. Rev.* **68**, 301 (2004).
30. D. S. Bischoff, G. W. Ordal. *Mol. Microbiol.* **6**, 23 (1992).
31. L. F. Garrity, G. W. Ordal. *Pharmacol. Ther.* **68**, 87 (1995).
32. V. M. Delgado-Nixon, G. Gonzalez, M.-A. Gilles-Gonzalez. *Biochemistry* **39**, 2685 (2000).
33. Y. Sasakura, S. Hirata, S. Sugiyama, S. Suzuki, S. Taguchi, M. Watanabe, T. Matsui, I. Sagami, T. Shimizu. *J. Biol. Chem.* **277**, 23821 (2002).
34. H. Takahashi, T. Shimizu. *Chem. Lett.* **35**, 970 (2006).
35. A. Tanaka, H. Takahashi, T. Shimizu. *J. Biol. Chem.* **282**, 21301 (2007).
36. T. G. Spiro, X.-Y. Li. *Biological Applications of Raman Spectroscopy*, Vol. 3, pp. 1–37, John Wiley, New York (1988).
37. M. Abe, T. Kitagawa, Y. Kyogoku. *J. Chem. Phys.* **69**, 4526 (1978).
38. T. G. Spiro, J. D. Stong, P. Stein. *J. Am. Chem. Soc.* **101**, 2648 (1979).
39. T. Kitagawa. In *Biological Applications of Raman Spectroscopy*, Vol. 3, T. G. Spiro (Ed.), pp. 97–130, Wiley-Interscience, New York (1988).
40. N.-T. Yu, E. A. Kerr. In *Biological Applications of Raman Spectroscopy*, Vol. 3, T. G. Spiro (Ed.), pp. 39–95, Wiley-Interscience, New York (1988).
41. I. Harada, H. Takeuchi. In *Spectroscopy of Biological Systems, Advances in Spectroscopy*, R. J. H. Clark, R. E. Hester (Eds.), pp. 113–175, John Wiley, Chichester, UK (1986).
42. J. C. Austin, T. Jordan, T. G. Spiro. In *Biomolecular Spectroscopy, Part A, Advances in Spectroscopy*, R. J. H. Clark, R. E. Hester (Eds.), pp. 55–127, John Wiley, Chichester, UK (1993).
43. H. Takeuchi. *Biopolymers* **72**, 305 (2003).
44. K. R. Rodgers, C. Su, S. Subramaniam, T. G. Spiro. *J. Am. Chem. Soc.* **114**, 3697 (1992).
45. Y. Gao, S. F. El-Mashtoly, B. Pal, T. Hayashi, K. Harada, T. Kitagawa. *J. Biol. Chem.* **281**, 24637 (2006).
46. M. Kubo, S. Inagaki, S. Yoshioka, T. Uchida, Y. Mizutani, S. Aono, T. Kitagawa. *J. Biol. Chem.* **281**, 11271 (2006).
47. S. F. El-Mashtoly, S. Yamauchi, M. Kumauchi, N. Hamada, F. Tokunaga, M. Unno. *J. Phys. Chem. B* **109**, 23666 (2005).
48. G. S. Kachalova, A. N. Popov, H. D. Bartunik. *Science* **284**, 473 (1999).
49. G. Gonzalez, E. M. Dioum, C. M. Bertolucci, T. Tomita, M. Ikeda-Saito, M. R. Cheesman, N. J. Watmough, M.-A. Gilles-Gonzalez. *Biochemistry* **41**, 8414 (2002).
50. A. Sato, Y. Sasakura, S. Sugiyama, I. Sagami, T. Shimizu, Y. Mizutani, T. Kitagawa. *J. Biol. Chem.* **277**, 32650 (2002).
51. T. Tomita, G. Gonzalez, A. L. Chang, M. Ikeda-Saito, M.-A. Gilles-Gonzalez. *Biochemistry* **41**, 4819 (2002).
52. S. Hirata, T. Matsui, Y. Sasakura, S. Sugiyama, T. Yoshimura, I. Sagami, T. Shimizu. *Eur. J. Biochem.* **270**, 4771 (2003).
53. S. F. El-Mashtoly, S. Nakashima, A. Tanaka, T. Shimizu, T. Kitagawa. *J. Biol. Chem.* **283**, 19000 (2008).
54. H. Kurokawa, D.-S. Lee, M. Watanabe, I. Sagami, B. Mikami, C. S. Raman, T. Shimizu. *J. Biol. Chem.* **279**, 20186 (2004).
55. H. J. Park, C. Suquet, J. D. Satterlee, C. Kang. *Biochemistry* **43**, 2738 (2004).
56. W. N. Lanzilotta, D. J. Schuller, M. V. Thorsteinnsson, R. L. Kerby, G. P. Roberts, T. L. Poulos. *Nat. Struct. Biol.* **7**, 876 (2000).

57. S. Taguchi, T. Matsui, J. Igarashi, Y. Sasakura, Y. Araki, O. Ito, S. Sugiyama, I. Sagami, T. Shimizu. *J. Biol. Chem.* **279**, 3340 (2004).
58. U. Liebl, L. Bouzahir-Sima, L. Kiger, M. C. Marden, J.-C. Lambry, M. Negrerie, M. H. Vos. *Biochemistry* **42**, 6527 (2003).
59. S. F. El-Mashtoly, H. Takahashi, T. Shimizu, T. Kitagawa. *J. Am. Chem. Soc.* **129**, 3556 (2007).
60. S. F. El-Mashtoly, H. Takahashi, H. Kurokawa, A. Sato, T. Shimizu, T. Kitagawa. *J. Raman Spectrosc.* **39**, 1614 (2008).
61. S. Crosson, S. Rajagopal, K. Moffat. *Biochemistry* **42**, 2 (2003).
62. M. Watanabe, H. Kurokawa, T. Yoshimura-Suzuki, I. Sagami, T. Shimizu. *Eur. J. Biochem.* **271**, 3937 (2004).
63. W. Zhang, G. N. Phillips. *Structure* **11**, 1097 (2003).
64. T. Ohta, H. Yoshimura, S. Yoshioka, S. Aono, T. Kitagawa. *J. Am. Chem. Soc.* **126**, 15000 (2004).
65. H. Yoshimura, S. Yoshioka, K. Kobayashi, T. Ohta, T. Uchida, M. Kubo, T. Kitagawa, S. Aono. *Biochemistry* **45**, 8301 (2006).
66. J. F. Cerda-Colon, E. Silfa, J. Lopez-Garriga. *J. Am. Chem. Soc.* **120**, 9312 (1998).
67. S. Hu, I. K. Morris, J. P. Singh, K. M. Smith, T. G. Spiro. *J. Am. Chem. Soc.* **115**, 12446 (1993).
68. E. S. Peterson, J. M. Friedman, Y. E. T. Chien, S. G. Sligar. *Biochemistry* **37**, 12301 (1998).
69. H. E. Van Wart, J. Zimmer. *J. Biol. Chem.* **260**, 8372 (1985).
70. S. F. El-Mashtoly, Y. Gu, H. Yoshimura, S. Yoshioka, S. Aono, T. Kitagawa. *J. Biol. Chem.* **283**, 6942 (2008).
71. K. M. Ottemann, W. Xiao, Y.-K. Shin, D. E. Koshland. *Science* **285**, 1751 (1999).
72. H. Szurmant, M. W. Bunn, S. H. Cho, G. W. Ordal. *J. Mol. Biol.* **344**, 919 (2004).